TÜBİTAK

Turkish Journal of Chemistry

http://journals.tubitak.gov.tr/chem/

Research Article

Turk J Chem
(2018) 42: 780 – 793

doi:10.3906/kim-1705-51

Electrochemical behavior and voltammetric determination of some nitro-substituted benzamide compounds

Özlem SAĞLAM[1], Ferah CÖMERT ÖNDER[2], Tuğba GÜNGÖR[2], Mehmet AY[2], Yusuf DİLGİN[1,*]

[1]Analytical Research Laboratory, Department of Chemistry, Faculty of Science and Arts, Çanakkale Onsekiz Mart University, Çanakkale, Turkey

[2]Natural Products and Drug Research Laboratory, Department of Chemistry, Faculty of Science and Arts, Çanakkale Onsekiz Mart University, Çanakkale, Turkey

Received: 29.05.2017 • **Accepted/Published Online:** 02.04.2018 • **Final Version:** 01.06.2018

Abstract: Voltammetric behaviors of six nitro-substituted benzamides, which are potential prodrug candidates for nitroreductase-based cancer therapy, were investigated using cyclic voltammetry (CV) and differential pulse voltammetry (DPV). The electrochemical behavior of aromatic nitro ($ArNO_2$) compounds by CV indicates that compounds involve various reduction/oxidation steps including the formation of aromatic nitro radical, nitroso, hydroxylamine, and amine groups. Applicability of the voltammetric determination of these prodrug candidates was studied by recording their DPVs, carried out in mixed media (Britton Robinson buffer solution + DMF) at various pH values on a pencil graphite electrode (PGE). Results show that the PGE can offer a disposable, low-cost, and sensitive electrochemical determination method for identifying nitro benzamide compounds. Under the experimental conditions, the PGE had a linear response range from 0.5 to 100 μM 4-nitro-*N*-(2-nitrophenyl)benzamide (compound **2**). This voltammetric procedure indicates that nitro-substituted benzamide drugs can be successfully determined in pharmaceutical samples.

Key words: Voltammetry, pencil graphite electrode, nitro-substituted benzamide compounds

1. Introduction

Nitro aromatic compounds ($ArNO_2$) have received considerable attention over recent decades as they are widely used as pesticides, explosives, pharmaceuticals, and chemical intermediates in industry due to their important functions such as pollutants and toxicants, in mutagenesis and carcinogenesis, and for their therapeutic actions.[1] Some of these compounds are potently toxic or carcinogenic, presenting a considerable danger to the human population, and are widely distributed environmental pollutants found in industrial regions. On the other hand, it is well known that many $ArNO_2$ compounds are widely used as prodrugs or drugs (e.g., chloramphenicol,[2] 5-(aziridine-1-yl)-2,4-dinitrobenzamide (CB1954),[3,4] nilutamide,[5] flutamide,[6] nimesulide,[7,8] ledakrin and derivatives of 1-nitro-9-aminoacridine[9,10] and niclosamide,[11] nitracrine, nitrazepam, nitrofurantoin, nitromersol, nitromide, and dinodeb[12]). These compounds have antihelminthic, antiprotozoal, and antibacterial properties that aid in combating a variety of protozoan and bacterial infections, as well as antitumor and anticancer, anticonvulsant, and antiinflammatory activities. Therefore, many researchers have focused on the synthesis and biological or therapeutic activity of new $ArNO_2$ compounds for these reasons.[13–21]

*Correspondence: ydilgin@yahoo.com

The therapeutic and biological activity mechanism of $ArNO_2$ compounds can be explained by their electrochemical behavior since the reduction of $ArNO_2$ compounds, which can accept up to six electrons to give the corresponding amino derivative, affects their biological activity. A useful review of $ArNO_2$ compounds related to their toxicity, carcinogenicity, mutagenicity, therapeutic functions, and mechanism was reported by Kovacic and Somanathan.[1] They stated that the mechanism is dependent on the electron transfer pathways of $ArNO_2$ compounds by the participation of nitroreductases, involving single-electron transfer leading to the formation of nitroxyl anion radical ($ArNO_2^{\cdot -}$), nitroso (ArNO), hydroxylamine (ArNHOH), and amine (Ar-NH_2) derivatives. These species have a cytotoxic effect on mammalian, protozoan, and bacterial cells.[1,22] Electrochemical techniques, especially cyclic voltammetry (CV), are very useful tools for obtaining information on the physical and chemical properties of electroactive molecules in organic electrochemistry. Electrochemical properties of biologically important compounds can be very valuable for elucidation of the main redox reactions that occur in the human body, providing a good approximation of what occurs in vivo. Therefore, electrochemical studies on $ArNO_2$ compounds have garnered much interest in recent years due to their above discussed properties.[23–39] In most of these studies, the electrochemical behavior of $ArNO_2$ compounds was explained by all nitro compounds reducing in two cathodic processes giving hydroxylamine and amine derivatives via reduction by four electrons and a further two electrons, respectively. It has also been reported that $ArNO_2$ compounds can generate a reversible single-electron process due to formation of $ArNO_2^{\cdot -}$ and an irreversible 3-electron process corresponding to formation of ArNHOH.[24]

In the current study, the electrochemical behaviors of six nitro-substituted benzamide compounds were investigated by means of a pencil graphite electrode (PGE). When compared with other carbon-based electrodes, PGEs have the same advantages, such as high electrochemical reactivity, commercial availability, good mechanical rigidity, disposability, low cost, low technology, and ease of modification.[40] In addition, it was reported that pencil lead electrodes offer a renewal surface that is simpler and faster than polishing procedures, common with solid electrodes, and result in good reproducibility for individual surfaces.[40] Thus, many scientists have recently focused on the use of this electrode in various electroanalytical applications due to the useful properties of PGEs.[38–43] Accordingly, a PGE was chosen as the electrode material in this study due to its important advantages including disposability, low cost, and renewable surface.[38–43] The effect of pH and scan rate on the reversible reduction oxidation of $ArNO_2$ to $ArNO_2^{\cdot -}$ and ArNHOH was investigated using CV. In addition, to assess these $ArNO_2$ compounds as potential prodrug candidates in cancer therapy or biological activities, differential pulse voltammetry (DPV) was also conducted.

2. Results and discussion

2.1. Cyclic voltammetric analysis of nitro benzamides

To investigate the electrochemical behavior of different $ArNO_2$ amide compounds (**1**–**6**) (Figure 1), cyclic voltammograms of each compound (with five repeated cycles) were recorded in Britton–Robinson buffer solution (BRBS) (pH 7.0) containing 0.1 M KCl and 30% DMF at a scan rate of 50 mV s^{-1} at the PGE (Figure 2). To elucidate the electrochemical mechanism, the potential was initially scanned from 0.1 to 0.8 V, then from 0.8 to –1.0 V, and finally from –1.0 to 0.1 V. Figures 2A–2F indicate that the electrochemical behaviors of the substituted benzamides containing different nitro groups show little differentiation from each other. For example, cyclic voltammograms of 4-nitro-*N*-(phenyl)-benzamide (compound **1**) are shown in Figure 2A. It has three reduction peaks and Ic_1 (–600 mV), IIc_1 (–90 mV), and IIIc (–690 mV) (Figure 2A) can be attributed to

the formation of one dihydroxylamine that immediately converted to hydroxylamine, the reduction of the nitroso group to hydroxyl amine, and the formation of amine, respectively. The reason for this is that it has only one NO_2 group. After the formation of dihydroxylamine (Ic_1), it immediately reduced to hydroxylamine since the hydroxylamine was reduced at a more positive potential (about –90 mV). Finally, the produced hydroxylamine reversibly oxidized to the nitroso group (IIa). On the other hand, the cyclic voltammogram of 4-nitro-*N*-(2-nitrophenyl)benzamide (compound **2**), containing two aromatic nitro groups, exhibits five reduction and three oxidation peaks. In the first scanning range (from 0.1 to 0.8 V) of the first cycle, an irreversible peak attributed to formation of radicals was not observed (Figure 2B). Peak potentials of all compounds are presented in Table 1. Cathodic peaks (IIc_1 and IIc_2 in Figure 2B), which appeared after the second cycle at about –70 and –130 mV, were not observed in the second scanning range (from 0.8 to –1.0 V) of the first cycle. In order to see these peaks, first dihydroxylamines and then hydroxylamines must be produced. Thus, two irreversible peaks were observed at –540 (Ic_1) and –625 (Ic_2) mV, in which two nitro groups were reduced to dihydroxylamine by accepting four electrons/four protons.

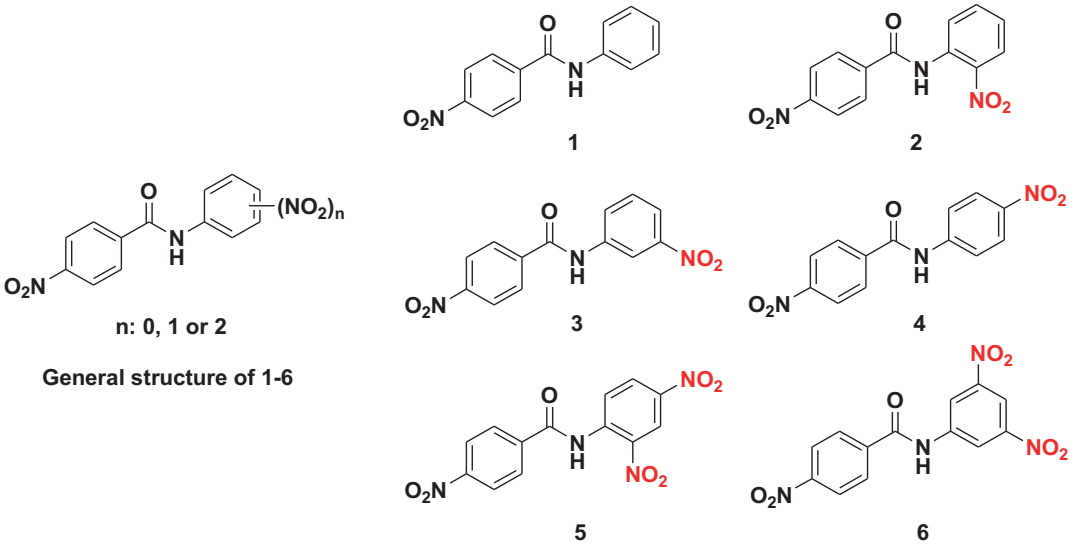

Figure 1. Structures of nitro aromatic compounds **1**–**6**.

The current of these irreversible reduction peaks decreased with an increase in the scan cycle. This is because the produced dihydroxylamines converted to a nitroso group by giving 2 mol of H_2O for two dihydroxylamines, following which the produced nitroso group immediately reduced to monohydroxylamine, accepting four electrons/four protons. In total, two -NO_2 groups in compound **2** were reduced to two monohydroxylamines by accepting eight electrons/eight protons. The produced monohydroxylamines converted to redox pairs (IIa_1/IIc_1 and IIa_2/IIc_2, Figure 2B) after the final scanning range (from –1.0 to 0.1 V), which can be attributed to the *N*-phenylhydroxylamines being oxidized to the nitroso group by the two-electron/two-proton process for one -NO_2 group (IIa_1 and IIa_2, Figure 2B).

On the other hand, the final reduction process including irreversible reduction of ArNHOH to $ArNH_2$ by accepting four electrons/four protons and giving 2 mol of H_2O (Figure 3) was observed as overlapping/superimposed with dihydroxylamine peaks in the first scanning range. It can be seen that the formation of amines (IIIc, Figure 2B) was observed to have more negative potential (–800 mV) than the formation of dihydroxylamines

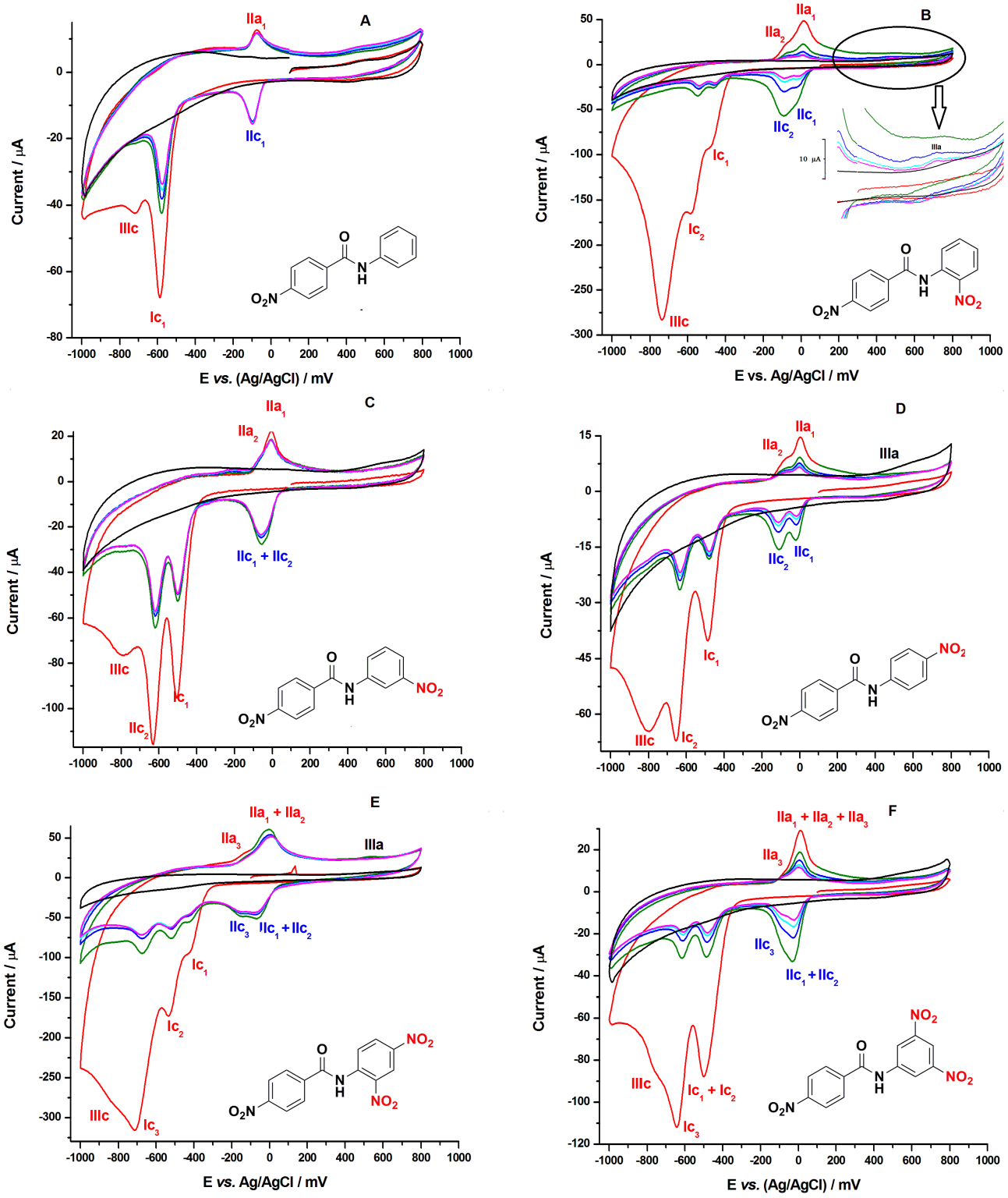

Figure 2. Cyclic voltammograms of 0.1 mM nitro benzamides (compounds **1** (A), **2** (B), **3** (C), **4** (D), **5** (E), and **6** (F)) for five successive cycles in BRBS (pH 7.0) containing 0.1 M KCl and 30% DMF. Red line is first cycle and other colored lines are successive cycles. Black line: CV of supporting electrolyte in the absence of compounds.

Table 1. Peak potentials of all reduction and oxidation peaks obtained from cyclic voltammograms of nitro benzamides recorded at PGE in BRBS (pH 7.0) containing 0.1 M KCl and 30% DMF.

Compounds	Peak potentials (mV)										
	Ic_1	Ic_2	Ic_3	IIa_1	IIa_2	IIa_3	IIc_1	IIc_2	IIc_3	IIIa	IIIc
1	–585			–75			–95				–715
2	–480	–580	-	15	–85	-	–25	–90	-	500 (small peak)	–735
3	–525	–655		0	–70		–15	–65		-	–800
4	–485	–655		0	–70		–20	-110		420	–800
5	–425	–535	–715	–5		–135	–65		–155	525	–835
6	–500		–645	10			–30		–90	550	–780

(–540 and –630 mV for Ic_1 and Ic_2, respectively). In addition, an irreversible peak attributed to the formation of one radical (IIIa, Figure 2B) was observed at 500 mV after the nitroso group was formed.

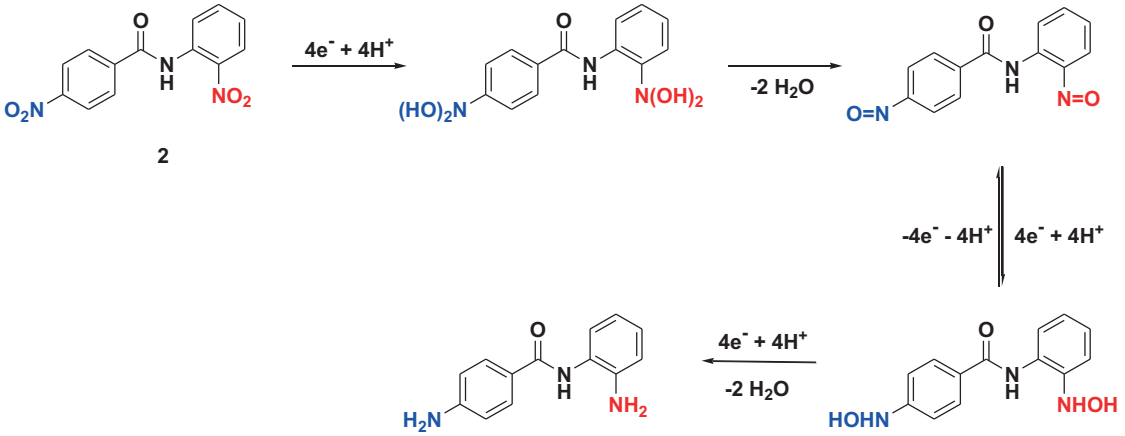

Figure 3. Proposed mechanism for electrochemical behavior of compound **2**.

These results can be interpreted by a mechanism proposed in the literature.[29,35] First, $ArNO_2$ groups are irreversibly reduced to $ArN(OH)_2$ by four electrons/four protons for two nitro groups. Then the produced $ArN(OH)_2$ groups convert to ArNO by giving 2 mol of H_2O, which are immediately reduced to ArNHOH by four electrons/four protons for two nitroso groups because the reduction potential of ArNHOH is more positive than that of $ArN(OH)_2$. Then ArNHOH is reversibly oxidized to ArNO by four electrons/four protons for two nitro groups (Figure 3). Finally, the produced ArNHOH is also irreversibly reduced to $ArNH_2$ by accepting four electrons/four protons and giving 2 mol of H_2O (Figure 3).

Similar results were also obtained from the cyclic voltammograms of 4-nitro-*N*-(3-nitrophenyl)benzamide (compound **3**) (Figure 2C) and 4-nitro-*N*-(4-nitrophenyl)benzamide (compound **4**) (Figure 2D). However, peaks of Ic_1, Ic_2, and IIIc for these two benzamides (compounds **3** and **4**) were observed separately, unlike the three peaks observed as overlapping or superimposed for compound **2**. In addition, IIa_1/IIc_1 and IIa_2/IIc_2 redox pairs appeared separately for compounds **2** and **4**, while they were observed as one peak for compound **3**.

Further experiments were also conducted on the benzamides including three nitro groups (compounds **5** and **6**). Cyclic voltammograms of 4-nitro-*N*-(2,4-dinitrophenyl)benzamide (compound **5**) and 4-nitro-*N*-(3,5-dinitrophenyl)benzamide (compound **6**) are shown in Figures 2E and 2F, respectively. Compound **5** has four reduction peaks and the first three peaks (Ic_1, Ic_2, and Ic_3) are attributed to the formation of three dihydroxylamines, representing three independent nitro groups on the molecule. The last peak (IIIc), which overlapped with Ic_3, represents the formation of $ArNH_2$ (Figure 2E). On the other hand, compound **6** has three reduction peaks for the formation of three dihydroxyl amines, whereas it also has three independent nitro groups (Figure 2F). As the nitro groups in the 3 and 5 positions of compound **6** have the same functions, their reduction to dihydroxylamines appeared as two peaks. A peak at about –480 mV is attributed to the combination of two reductions of nitro groups (Ic_1 + Ic_2) because the nitro groups in the 3 and 5 positions have some properties. Another peak observed at –630 mV is attributed to the reduction of the last nitro group (Ic_3) and the peak for the formation of $ArNH_2$ (IIIc) overlapped with this reduction peak. In addition, anodic peak currents for the oxidation of hydroxylamines to nitroso groups (IIa_1, IIa_2, and IIa_3) were observed as one peak, and the reduction of nitroso groups to hydroxylamines (IIc_1, IIc_2, and IIc_3) was observed as two peaks. These results show that the structure of benzamides can affect the electrochemical behavior of nitro groups.

2.2. Effect of pH on electrochemical behavior of nitro benzamides

To investigate the effect of pH on electrochemical responses (especially peak potential) of the nitro benzamide compounds at the PGE, cyclic voltammograms of each compound were recorded in BRBS containing 0.1 M KCl and 30% DMF at pH values ranging between 2.0 and 10.0 at a scan rate of 50 mV s^{-1}. Cyclic voltammograms of each compound recorded at different pH levels are shown in Supplementary Figures S1A, S1B, and S1C. The dependence of the peak potentials of each compound on pH are also shown in Supplementary Figure S2. The pH-potential curve of compound **1** (Supplementary Figure S2A) shows that peak potential decreases linearly with the increasing of pH. Similar behavior was observed for all compounds. For example, the reduction (Ic_1, Ic_2, IIc_1, and IIc_2) and oxidation (IIa_1, IIa_2, and IIIa) peak potentials for compound **2** (Supplementary Figure S2B) shifted to negative values with an increase of pH from 2.0 to 10.0. Linearity changes were observed with a slope of 40 mV for the reduction of Ic_1 and Ic_2, and also a slope of about 55 mV/pH for the other reduction (IIc_1 and IIc_2) and oxidation (IIa_1, IIa_2, and IIIa) peaks at pH values between 2.0 and 7.0.

However, it was observed that other dinitro compounds (compounds **3** and **4**) have slightly different curves for all peaks compared to the curves of compound **2** (Supplementary Figures S2C and S2D). For example, linearity ranges were observed at pH values between 2.0 and 6.0 and also a pH-potential curve was not obtained for IIIa of compound **3** (and also compound **6**) due to its disappearance in the cyclic voltammograms. pH-potential curves of the trinitro benzamide compounds are presented in Supplementary Figures S2E and S2F for compounds **5** and **6**, respectively. As can be seen, all peak potentials of these compounds shifted to negative values when pH increased from 2.0 to 10.0. The reason for the shift of cathodic peak potentials toward more negative values with increasing pH is that the nitro group accepted electrons more easily at low pH values because protonation of the nitro group causes a decrease in electron density in the NO_2 group region. On the other hand, electron transfer from the NO_2 group to the electrode for anodic peaks is easier at high pH values.

The linearity ranges of each oxidation and reduction peak were obtained from the pH-peak potential curves. The equations for well-defined straight lines of each reduction and oxidation peak are summarized in Table 2 for each compound. The peak potentials of reversible peaks (IIa_1/IIc_1, IIa_2/IIc_2, or IIa_1 + IIa_2/IIc_1

+ IIc_2), irreversible reduction peaks (Ic_1 and Ic_2), and the irreversible oxidation peak (IIIa) were pH-dependent with a slope changing between –40 and –63 mV per pH (Table 2), which is close to the anticipated Nernstian value of –59.16 mV. Therefore, it can be said that equal numbers of electrons and protons are transferred in the electrochemical reduction of Ar-NO_2 to Ar-$N(OH)_2$ ($2e^-/2H^+$ for one NO_2 group), oxidation of the produced Ar-NHOH to Ar-NO ($2e^-/2H^+$ for one NO_2 group), and also irreversible reduction of Ar-NO to Ar-$NHO^{\bullet-}$ ($1e^-/1H^+$ for one NO_2 group).

Table 2. Equations of peaks obtained from linear plot of pH versus potential of compounds **1**–**6**.

Peak	Compound **1**	Compound **2**	Compound **3**	Compound **4**	Compound **5**	Compound **6**
	pH 2–7		pH 2–6			
Ic_1	y = –53x – 174 R^2 = 0.9819	y = –40x – 258 R^2 = 0.9951	y = –41x – 297 R^2 = 0.9906	y = –49x – 230 R^2 = 0.9934	y = –43x – 131 R^2 = 0.9988	y = –52x – 199 R^2 = 0.9957
Ic_2	-	y = –40x – 347 R^2 = 0.9988	y = –46x – 351 R^2 = 0.9911	y = –51x – 372 R^2 = 0.9915	y = –58x – 152 R^2 = 0.9773	y = –59x – 312 R^2 = 0.9996
Ic_3	-	-	-	-	y = –85x – 182 R^2 = 0.9708	-
IIa_1	y = –63x + 419 R^2 = 0.9946	y = –56x + 342 R^2 = 0.9951	y = –57x + 345 R^2 = 0.9985	y = –59x + 353 R^2 = 0.9928	y = –55x + 343 R^2 = 0.9957	y = –56x + 349 R^2 = 0.9940
IIa_2	-	y = –56x + 268 R^2 = 0.9956		y = –57x + 236 R^2 = 0.9972		
IIa_3	-	-	-			
IIc_1	y = –60x + 375 R^2 = 0.9906	y = –56x + 316 R^2 = 0.9933	y = –60x + 318 R^2 = 0.9964	y = –58x + 334 R^2 = 0.9908	y = –55x + 343 R^2 = 0.9957	y = –60x + 339 R^2 = 0.9953
IIc_2	-	y = –54x + 250 R^2 = 0.9933		y = –60x + 246 R^2 = 0.9926		
IIc_3	-	-	-	-	y = –58x + 323 R^2 = 0.9950	-
IIIa	-	y = –49x + 758 R^2 = 0.9901	-	y = –46x + 715 R^2 = 0.9939	y = –63x + 760 R^2 = 0.9927	-

However, the peak potential of the irreversible reduction peaks (Ic_3) for compound **5** was pH-dependent with a slope of –85 mV per pH, indicating that the peak for the formation of Ar-NH_2 may affect this peak. The peak for the reduction of ArNHOH to $ArNH_2$ was not evaluated due to its instability. The pH experiment showed a general trend of decreasing reduction and oxidation peak potentials as the pH increased, indicating the involvement of hydronium ions in the whole reduction and oxidation process toward nitro-substituted benzamides.

2.3. Effect of scan rate on electrochemical behavior of nitro benzamides

In order to observe the effect of scan rate on peak currents of the nitro benzamides, cyclic voltammograms of compound **3** were selected (0.1 M BRBS at pH 7.0 containing 30% DMF and 0.1 M KCl) and were recorded at various scan rates using the PGE. The cyclic voltammograms for the first and second cycles of compound **3** dependent on scan rate are shown in Supplementary Figure S3. These cyclic voltammograms demonstrate that the oxidation peak potential of ArNHOH to Ar(N=O) (IIa_1 + IIa_2) shifts in a positive direction, while the

reduction peaks attributed to the formation of $ArN(OH)_2$ (Ic_1 and Ic_2) and ArNHOH (IIc_1 + IIc_2) shift in a somewhat negative direction with an increase of scan rate, indicating the kinetic limitations of the reduced process. The peak currents of IIa_1 + IIa_2, IIc_1 + IIc_2, Ic_1, and Ic_2 dependent scan rates were calculated from the second cycle. With an increase of scan rate, all peak currents varied linearly as the square root of the scan rate (Figure 4). These results manifested a typical diffusion-controlled electrochemical process. Similar behavior was also obtained for the other nitro compounds.

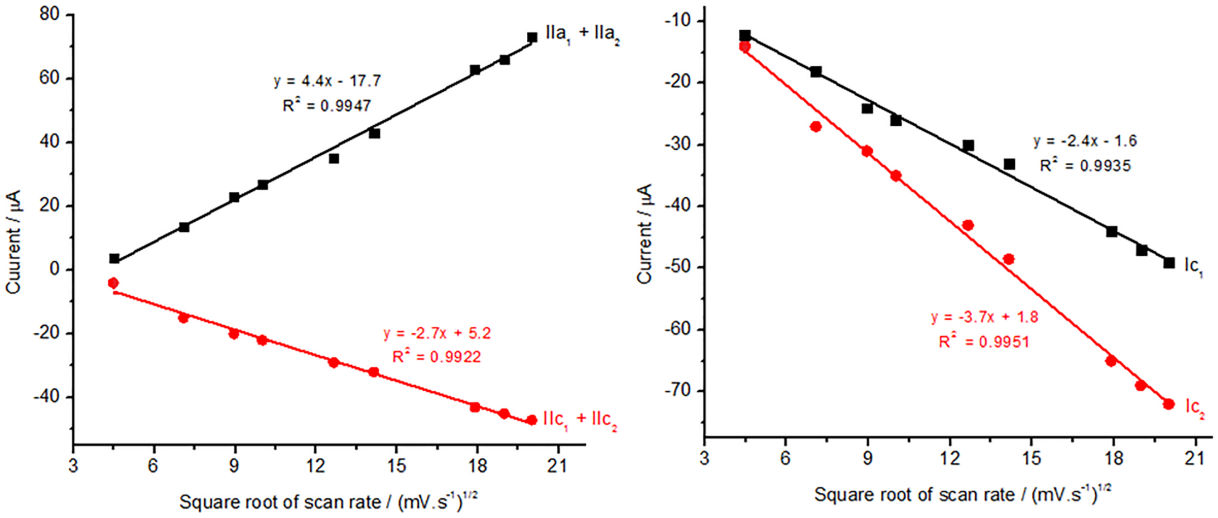

Figure 4. Plot of peak currents of compound **3** versus square root of scan rate.

2.4. Differential pulse voltammetric determination of nitro benzamides

In order to verify the practical applicability of the voltammetric determination of compounds **1**–**6**, compound **2** was selected as a model nitro benzamide for the monitoring of its differential pulse (DP) voltammogram. The influence of pH on the DP voltammetric behavior of 1.0 mM compound **2** at the PGE was investigated in BRBS containing 0.1 M KCl and 30% DMF at pH values ranging between 2.0 and 9.0. To observe the oxidation of the produced ArNHOH to Ar-NO with $4e^-$ (for two nitro groups), its DP voltammograms were recorded in the potential range of –500 mV to 500 mV. It can be seen from Figure 5A that compound **2** gives two anodic peaks, corresponding to the oxidation of ArNHOH to the ArNO group over the whole pH region. Figure 5B shows that the highest peak current was obtained at pH 7.0. Therefore, BRBS with pH 7.0 containing 0.1 M KCl and 30% DMF was used as the supporting electrolyte for subsequent DP voltammetric experiments.

To examine the relationship between anodic peak current corresponding to the oxidation of ArNHOH to the ArNO group, DP voltammograms of compound **2** were recorded in BRBS (pH 7.0) containing 0.1 M KCl and 30% DMF. Figure 6 shows the DP voltammograms at the PGE for various concentrations of compound **2**. A linear response was observed in the range between 0.5 and 100 μM (y (μA cm^{-2}) = 1.7x (μM) + 15.9, R^2 = 0.9901) (Figure 6, inset). The limit of detection (LOD) and limit of quantification (LOQ) were calculated by evaluation of the peak current for the smallest observable concentration of compound **2**. LOD and LOQ values were found to be 0.16 μM and 0.52 μM, respectively, using the equations of LOD = $3S_b$ / m and LOQ = $10S_b$ / m, where S_b is the standard deviation of the concentration of compound **2** (0.1 μM) and $m$is the slope of the calibration plot (1.7 μA μM^{-1} cm^{-2}).

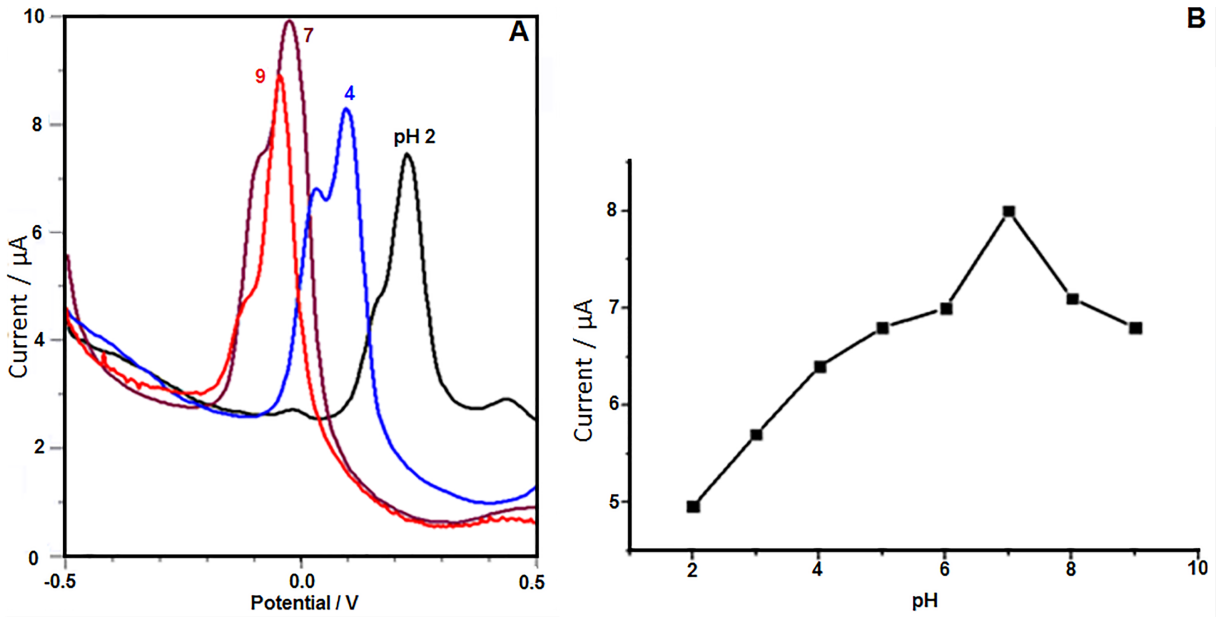

Figure 5. A) Differential pulse voltammograms of 5.0 μM compound **2** in BRBS with different pH values containing 0.1 M KCl and 30% DMF (pulse amplitude: 20 mV, pulse time: 30 s, scan rate: 25 mV s^{-1}). B) Plot of peak current of compound **2** versus pH.

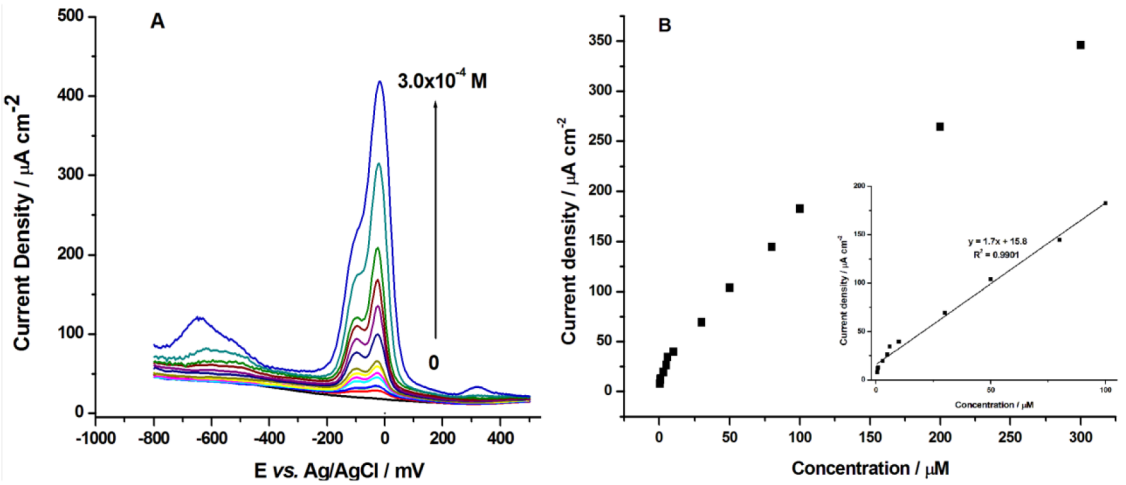

Figure 6. A) Differential pulse voltammograms of compound **2** at PGE in BRBS (pH 7.0) containing 0.1 M KCl and 30% DMF for different concentrations of compound **2** (pulse amplitude: 20 mV, pulse time: 30 s, scan rate: 25 mV s^{-1}). B) Plot of peak current of compound **2** versus concentration. Inset: Calibration curve for compound **2**.

The proposed electrode was used for the determination of compound **2**, which was selected as a model compound in spiked urine and also artificial prepared blood serum samples. Artificial blood serum samples were prepared according to the literature[44] without including compound **2**. For this, DP voltammograms were recorded by spiking a known volume and concentration of compound **2** standard solutions into the urine and artificial blood serum samples to obtain various concentrations. The obtained recovery results (Table 3) show that acceptable recoveries were obtained for spiked compound **2** in urine and artificial blood serum samples. These results indicate that nitro benzamide drugs can be successfully determined in pharmaceutical samples.

Table 3. The results of recovery studies for determination of compound **2** in urine and artificial blood serum samples (n = 3).

Sample	Added / μM	Found / μM	Recovery %
Urine	0	0	
	15.0	14.5 ± 0.8	96.7
	30.0	30.2 ± 1.2	100.7
Artificial blood serum	0	0	
	15.0	15.4 ± 0.3	102.7
	30.0	30.3 ± 1.1	101.0

The sensitivity and linearity ranges of the proposed method were compared with other bare or modified electrodes in previously published reports for electrochemical detection of aromatic nitro compounds (Table 4). The sensitivity and linearity range of the proposed method for determination of compound **2** was found to be 1.7 μA cm^{-2} L μmol^{-1} and 0.5–100 μM, respectively. As can be seen in Table 4, the linearity range is wider than that for the DP voltammetric determination of nitrofurantoin (NF) at a mercury meniscus modified silver solid amalgam electrode (2–100 μM),[36] determination of 2-amino-6-nitrobenzothiazole (ANBT) at a silver solid amalgam electrode modified by a microcrystalline natural graphite polystyrene composite film (0.2–10 μM),[33] amperometric detection of nitrophenol (NP) at a porous copper modified PGE (50–850 μM),[38] and cyclic voltammetric determination of trinitrotoluene (TNT) (2.5–40 and 40–120 mg L^{-1}) and dinitrotoluene (DNT) (2–40 and 40–140 mg L^{-1}).[30,31] The sensitivity of the proposed method is higher than that of determination of NF,[36] ANBT and 5-nitrobenzimidazole (5-NBIA),[33] NP,[38] TNT, and DNT.[30,31] Moreover, it is comparable to that obtained with determination of niclosamide at a PGE[39] and determination of aromatic nitro compounds (nitrobenzene, TNT, and DNT) at a Pd nanoparticle graphene modified GCE.[34]

Therefore, it can be said that PGE is very useful electrode material for investigation of the electrochemical behavior of aromatic nitro compounds, and also their determination, due to PGE having important advantages in terms of high electrochemical reactivity, commercial availability, good mechanical rigidity, disposability, low cost, low technology, ease of modification, lack of need for polishing, and a renewable surface.

In conclusion, an investigation on the electrochemical behavior of several nitro benzamides, prodrug candidates for nitroreductase-based cancer therapy, was presented in this study. The reduction and oxidation processes for all compounds changed depending on the pH of the experimental setups. Peak potential of all peaks decreased with increasing pH, with a slope near the anticipated Nernstian value of –59.16 mV. Therefore, it can be said that equal numbers of electrons and protons are transferred in all the electrochemical reduction and oxidation processes. We successfully created an extremely low-cost, disposable, and practical nitro benzamide sensor to record their DP voltammograms. This result indicates that nitro benzamides in drugs or pharmaceutical samples can easily be determined by the DP voltammetric procedure.

3. Experimental

3.1. Apparatus and chemicals

All electrochemical experiments were carried out using a CompactStat Electrochemical Interface (Ivium Technologies, Eindhoven, the Netherlands). Cyclic and DP voltammetric experiments were carried out in a 10-mL

Table 4. Comparison of analytical parameters of compound **2** at PGE with some electrodes in the literature for electrochemical detection of various aromatic nitro compounds.

Used modified electrode	Methodology	Compound	LR	LOD / LOQ	Ref.
Pretreated GCE	CV in MeCN including 0.04 M Bu_4NBr	1,3,5-Trinitro-1,3,5-triaza cyclohexane (RDX)	30.0–120.0 mg L^{-1}	10.2 / 20.6 mg L^{-1}	30
		Octahydro-1,3,5,7-tetranitro-1,3,5,7-tetrazocine (HMX)	40.0–120.0 mg L^{-1}	11.7 / 29.6 mg L^{-1}	
		Trinitrotoluene (TNT)	40.0–120.0 mg L^{-1}	11.2 / 23.0 mg L^{-1}	
		Dinitrotoluene (DNT)	40.0–140.0 mg L^{-1}	10.8 / 26.7 mg L^{-1}	
Gold nanoparticles/poly (*o*-phenylene diamine-aniline) film modified glassy carbon electrode	CV in MeCN:H_2O (5:95%) including 0.04 M NaCl	TNT	2.5–40.0 mg L^{-1}	2.1 / 7.0 mg L^{-1}	31
		DNT	2.0–40.0 mg L^{-1}	1.3 / 4.0 mg L^{-1}	
		Tetryl	5.0–100.0 mg L^{-1}	3.8 / 12.6 mg L^{-1}	
A silver solid amalgam electrode modified by a microcrystalline natural graphite–polystyrene composite film	Direct current voltammetry (DCV) and differential pulse voltammetry in a) MeOH-BR buffer pH 4.0 (1:9) for ANBT, b) MeOH-BR buffer pH 7.0 (1:9) for 5-NBIA	2-Amino-6-nitrobenzo thiazole (ANBT)	0.2–10.0 µM	Reduction DCV: - / 0.89 µM DPV: - / 0.77 µM	33
		5-Nitrobenz imidazole (5-NBIA)	0.2–10.0 µM	Reduction DCV: - / 0.62 µM DPV: - / 0.31 µM	
Pd nanoparticles on functionalized graphene modified GCE	DPV in 0.2 M PBS and 0. 5 M NaCl	Nitrobenzene	1.0–170.0 ppb	0.62 ppb / -	34
Mercury meniscus modified silver solid amalgam electrode	DCV and differential pulse voltammetry in methanol-BR buffer pH 7.0 (1:9)	Nitrofurantoin	DCV: 6.0–100.0 µM DPV: 0.2–100.0 µM	DCV: - / 1.6 µM DPV: - / 0.081 µM	36
Porous copper-modified graphite pencil electrode	Amperometric detection in pH 4.8 acetate buffer solution at –500 mV	4-Nitrophenol	50.0–850.0 µM	1.91 µM / -	38
Pencil graphite electrode	DPV in pH 7.0 BR buffer solution containing 0.1 M KCl and 30% DMF	Niclosamide	0.05–10.0 µM	0.015 µM / -	39
Pencil graphite electrode	DPV in pH 7.0 BR buffer solution containing 0.1 M KCl and 30% DMF	4-Nitro-*N*-(2-nitrophenyl)benza mide as a model compound	0.5–100.0 µM	0.16 / 0.52 µM	This work

voltammetric cell at room temperature (25 °C) using the traditional three-electrode system. A platinum wire, an $Ag/AgCl/KCl_{sat}$, and a PGE were used as the counter, reference, and working electrodes, respectively. The properties of the PGE were described in our previous work.[39] The 2B pencil graphite was obtained from Tombow (Japan) and consisted of 74% graphite and 20% clay. Its electrical resistance was measured and found to be about 0.5 ohm cm^{-1}. It offers very little electrical resistance, which does not produce a significant ohmic drop in the CV responses. This indicates that the PGE is a good candidate for electrode material. For each measurement, a total of 10 mm of lead (active electrode area was calculated as 0.159 cm^2) was immersed into the solution. An HI 221 Hanna pH meter with a combined glass electrode (Hanna HI 1332) was used to follow the pH values of the solutions. All solutions were prepared with ultrapure water from an Elga Option Q7B water purification system (18.2 MΩ cm).

4-Nitrobenzoyl chloride (98%), nitro-substituted anilines, magnesium sulfate (≥99.5%), sodium carbonate (≥99.0%), triethylamine and pyridine (for HPLC purity, ≥99.5%), benzene (for HPLC purity, ≥99.9%), H_3PO_4 (85%, d: 1.71 g mL^{-1}), CH_3COOH (96%, d: 1.05 g mL^{-1}), H_3BO_3, NaOH, and KCl were purchased from Sigma-Aldrich and all solvents were supplied by Merck. Dimethyl formamide (DMF) was purchased from Sigma (USA). BRBS in the pH range of 2–10 was prepared from 0.04 M H_3PO_4, 0.04 M H_3BO_3, and 0.04 M CH_3COOH containing 0.1 M KCl in deionized water. The pH of the solutions was adjusted by adding 0.2 M NaOH containing 0.1 M KCl.

3.2. Synthesis of nitro-substituted benzamide compounds

Six different nitro benzamide compounds, 4-nitro-*N*-(phenyl)-benzamide (**1**), 4-nitro-*N*-(2-nitrophenyl)benzamide (**2**), 4-nitro-*N*-(3-nitrophenyl)benzamide (**3**), 4-nitro-*N*-(4-nitrophenyl)benzamide (**4**), 4-nitro-*N*-(2,4-dinitrophenyl)benzamide (**5**), and 4-nitro-*N*-(3,5-dinitrophenyl)benzamide (**6**), were synthesized according to the literature[45–49] with some modifications and their structures were confirmed with ^1H NMR and ^{13}C NMR. The purity of compounds was determined according to NMR data.

3.3. Electrochemical procedure

The electrochemical behavior of the $ArNO_2$ compounds (**1**–**6**) was investigated by recording their cyclic voltammograms at the PGE in BRBS in the pH range of 2.0–10.0 containing 30% DMF and 0.1 M KCl. We placed 10 mL of supporting electrolyte containing 30% DMF and 0.1 M KCl in the electrochemical cell and 10 mm of pencil graphite was immersed into the supporting electrolyte. Cyclic voltammograms were recorded at a scan rate of 50 mV s^{-1} using a potential applied profile with two stop crossing, in which the potential was initially scanned from 0.1 V to 0.8 V, then from 0.8 V to –1.0 V, and finally from –1.0 to 0.1 V. Then the cyclic voltammograms of the PGE were recorded in the presence of 1.0×10^{-4} M $ArNO_2$ under the same experimental conditions after the required volume of 0.01 M stock solution of $ArNO_2$ was added to the cell. Cyclic voltammograms of each $ArNO_2$ were also recorded at various scan rates. High purity argon was used to purge the supporting electrolyte for 5 min before all electrochemical experiments.

Following this, the DP voltammetric technique was used for determination of $ArNO_2$ compounds, as in several biological and medical applications. First, the effect of pH on the DP voltammograms of each 2.5×10^{-5} M $ArNO_2$ compound was investigated. DP voltammograms were recorded in a potential range between –0.8 V and 0.4 V at a scan rate of 25 mV s^{-1} and using optimized pulse amplitude (20 mV) and pulse time (30 ms). After each successive DP voltammetric measurement, argon gas purged the supporting electrolyte for 20 s prior to the next measurement.

DP voltammetric determination of compound **2** was performed in two different samples, urine and artificial blood serum, which were prepared according to literature[44]. Urine samples were obtained from a healthy volunteer and filtered with a membrane filter. Spiked samples were prepared by mixing the proper amount of sample solutions with a known concentration of compound **2**. Then DP voltammograms were recorded for each sample under conditions described in Figure 6.

Acknowledgment

This work was partially supported by the Scientific and Technological Research Council of Turkey (TÜBİTAK 1001, Grant No. 110T754). The authors wish to thank TÜBİTAK for this financial support.

References

1. Kovacic, P.; Somanathan, R. *J. Appl. Toxicol.* **2014**, *34*, 810-824.
2. Rheingold, J. J.; Spurling, C. L. *J. Am. Medical. Assoc.* **1952**, *149*, 1301-1304.
3. Helsby, N.; Wheeler, S. J.; Pruijjn, F. B.; Palmer, B. D.; Yang, S.; Denny, W. A.; Wilson, W. R. *Chem. Res. Toxicol.* **2003**, *16*, 469-478.
4. Knox, R. J.; Friedlos, F.; Biggs, P. J.; Flitter, W. D.; Gaskell, M.; Goddard, P.; Davies, L.; Jarman, M. *Biochem. Pharmacol.* **1993**, *46*, 797-803.
5. Ask, K.; Dijols, S.; Giroud, C.; Casse, L.; Frapart, Y. M.; Sari, M. A.; Kim, K. S.; Stuehr, D. J.; Mansuy, D.; Camus, P. et al. *Chem. Res. Toxicol.* **2003**, *16*, 1547-1554.
6. Coe, K. J.; Jia, Y.; Ho, H. K.; Rademacher, P.; Bammler, T. K.; Beyer, R. P.; Farin, F. M.; Woodke, L.; Plymate, S. R.; Fausto, N. et al. *Chem. Res. Toxicol.* **2007**, *20*, 1277-1290.
7. Zhong, B.; Cai, X.; Chennamaneni, S.; Yi, X.; Liu, L.; Pink, J. J.; Dowlati, A.; **Xu**, Y.; Zhou, A.; Su, B. *Eur. J. Med. Chem.* **2012**, *47*, 432-444.
8. Al-Abd, A. M.; Al-Abbasi, F. A.; Nofal, S. M.; Khalifa, A. E.; Williams, R. O.; El-Eraky, W. I.; Nagy, A. A.; Abdel-Naim, A. B. *PLoS One* **2014**, *9*, e111843.
9. Woynarowski, J. M.; Bartoszek, A.; Konopa, J. *Chem. Biol. Interact.* **1984**, *49*, 311-328.
10. Gorlewska, K.; Mazerska, Z.; Sowiński, P.; Konopa, J. *Chem. Res. Toxicol.* **2001**, *14*, 1-10.
11. Pan, J. X.; Ding, K.; Wang, C. Y. *Chin. J. Cancer*, **2012**, *31*, 178-184.
12. O'Neil, M. J. The Merck Index. 14th ed. Merck Research Laboratories: Whitehouse Station, NJ, USA, 2006, pp. 1136-1146.
13. Lopes, M. S.; de Souza Pietra, R. C. C.; Borgati, T. F.; Romeiro, C. F. D.; Júnior, P. A. S.; Romanha, A. J.; Alves, R. J.; Souza-Fagundes, E. M.; Fernandes, A. P. S. M.; de Oliveira, R. B. *Eur. J. Med. Chem.* **2011**, *46*, 5443-5447.
14. Serafim, R. A. M.; Gonçalves, J. E.; de Souza, F. P.; de Melo Loureiro, A. P.; Storpirtis, S.; Krogh, R.; Andricopulo, A. D.; Dias, L. C.; Ferreira, E. I. *Eur. J. Med. Chem.* **2014**, *82*, 418-425.
15. Papadopoulou, M. V.; Trunz, B. B.; Bloomer, W. D.; McKenzie, C.; Wilkinson, S. R.; Prasittichai, C.; Brun, R.; Kaiser, M.; Torreele, E. *J. Med. Chem.* **2011**, *54*, 8214-8223.
16. Badr, S. M. I.; Barwa, R. M. *Bioorg. Med. Chem.* **2011**, *19*, 4506-4512.
17. **Supuran**, C. T. *Expert Opin. Ther. Pat.* **2012**, *22*, 1251-1255.
18. Tiwari, R.; Mollmann, U.; Cho, S.; Franzblau, S. G.; Miller, P. A.; Miller, M. J. *ACS Med. Chem. Lett.* **2014**, *5*, 587-591.
19. Curtis, B.; Payne, T. J.; Ash, D. E.; Mohanty, D. K. *Bioorg. Med. Chem.* **2013**, *21*, 1123-1135.

20. Narayana, B.; Ashalatha, B. V.; Vijaya Raj, K. K.; Fernandes, J.; Sarojini, B. K. *Bioorg. Med. Chem.* **2005**, *13*, 4638-4644.
21. Kulkarni, R. G.; Laufer, S. A.; Chandrashekhar, V. M.; Garlapati, A. *Med. Chem.* **2013**, *9*, 91-99.
22. Kovacic, P.; Osuna, J. A. *Curr. Pharm. Design* **2006**, *6*, 277-309.
23. Carbajo, J.; Bollo, S.; Nunez-Vergara, L. J.; Navarrete, P.; Squella, J. A. *J. Electroanal. Chem.* **2000**, *494*, 69-76.
24. Nunez-Vergara, L. J.; Bonta, M.; Navarrete-Encina, P. A.; Squella, J. A. *Electrochim. Acta* **2001**, *46*, 4289-4300.
25. Chapuzet, J. M.; Gru, C.; Labrecque, R.; Lessard, J. *J. Electroanal. Chem.* **2001**, *507*, 22-29.
26. Carbajo, J.; Bollo, S.; Nunez-Vergara, L. J.; Campero, A.; Squella, J. A. *J. Electroanal. Chem.* **2002**, *531*, 187-194.
27. Fotouhi, L.; Faramarzi, S. *J. Electroanal. Chem.* **2004**, *568*, 93-99.
28. Peckova, K.; Barek, J.; Navratil, T.; Yosypchuk, B.; Zima, J. *Anal. Lett.* **2009**, *42*, 2339-2363.
29. Chua, C. K.; Pumera, M. *Electroanalysis* **2011**, *23*, 2350-2356.
30. Üzer, A.; Sağlam, Ş.; Tekdemir, Y.; Ustamehmetoğlu, B.; Sezer, E.; Erçağ, E.; Apak, R. *Talanta* **2013**, *115*, 768-778.
31. Sağlam, Ş.; Üzer, A.; Tekdemir, Y.; Erçağ, E.; Apak, R. *Talanta*, **2015**, *139*, 181-188.
32. Andres, T.; Eckmann, L.; Smith, D. K. *Electrochim. Acta* **2013**, *92*, 257-268.
33. Deylova, D.; Vyskocil, V.; Barek, J. *J. Electroanal. Chem.* **2014**, *717-718*, 237-242.
34. Zhou, X.; Yuan, C.; Qin, D.; Xue, Z.; Wang, Y.; Du, J.; Ma, L.; Ma, L.; Lu, X. *Electrochim. Acta* **2014**, *119*, 243-250.
35. Panchompoo, J.; Aldous, L.; Compton, R. G. *New J. Chem.* **2010**, *34*, 2643-2653.
36. Krejcova, Z.; Barek, J.; Vyskocil, V. *Electroanalysis* **2015**, *27*, 185-192.
37. Bollo, S.; Nunez-Vergara, L. J.; Squella, J. A. *J. Electroanal. Chem.* **2004**, *562*, 9-14.
38. Kawde, A. N.; Aziz, M. A. *Electroanalysis* **2014**, *26*, 2484-2490.
39. Dede, E.; Sağlam, Ö.; Dilgin, Y. *Electrochim. Acta* **2014**, *127*, 20-26.
40. Wang, J.; Kawde, A. N.; Sahlin, E. *Analyst* **2000**, *125*, 5-7.
41. Dilgin, Y.; Kızılkaya, B.; Ertek, B.; Işık, F.; Dilgin, D. G. *Sens. Actuators B* **2012**, *171-172*, 223-229.
42. Dilgin, Y.; Kızılkaya, B.; Dilgin, D. G.; Gökçel, H. İ.; Gorton, L. *Colloids Surf. B* **2013**, *102*, 816-821.
43. Uygun, Z. O.; Dilgin, Y. *Sens. Actuators B* **2013**, *188*, 78-84.
44. Özcan, H.M., Sezgintürk, M.K. *Biotechnol. Prog.* 2015, *31,* 815-822.
45. Kamal, A.; Reddy, K. S.; Khan, M. N.; Shetti, R. V.; Ramaiah, M. J.; Pushpavalli, S. N.; Srinivas, C.; Pal-Bhadra, M.; Chourasia, M.; Sastry, G. N. et al. *Bioorg. Med. Chem.* **2010**, *18*, 4747-4761.
46. Tümer, T. B.; Önder, F. C.; İpek, H.; Güngör, T.; Savranoğlu, S.; Tok, T. T.; Çelik, A.; Ay, M. *Int. Immunopharmacol.* **2017**, *43*, 129-139.
47. Furniss, B. S.; Hannaford, A. J.; Smith, P. W. G.; Tatchell, A. R. In: Vogel, I.; Furniss, B. S.; Smith, P. W., Eds. *Vogel's Textbook of Practical Organic Chemistry*; Longman: London, UK, 1978, pp. 1130-1131.
48. Al-Shawabkeh, D.; Al-Nadaf, A. H.; Dahabiyeh, L. A.; Taha, M. O. *Med. Chem. Res.* **2014**, *23*, 127-145.
49. Sun, Y.; Wang, G.; Guo, W. *Tetrahedron* **2009**, *65*, 3480-3485.

Supplementary data

Electrochemical behavior and voltammetric determination of some nitro-substituted benzamide compounds

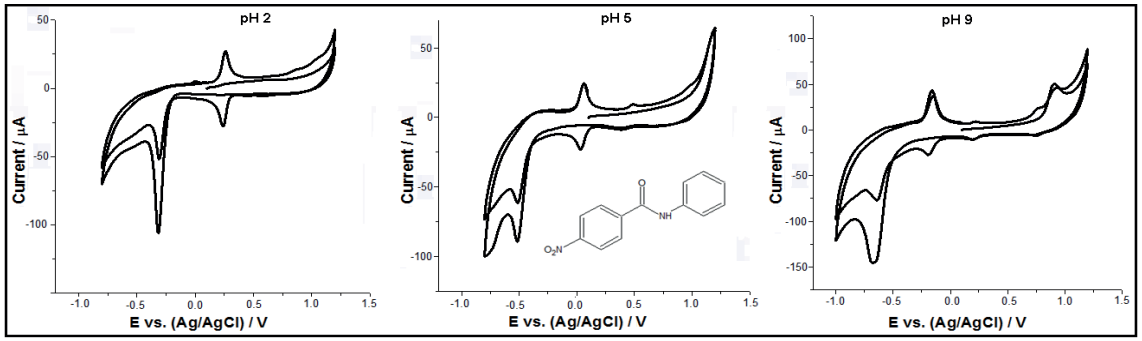

Figure S1A. Cyclic voltammograms of 0.1 mM mononitro benzamide for five successive cycles in BRBS (pH of 2, 5, and 9) containing 0.1 M KCl and 30% DMF (compound **1**).

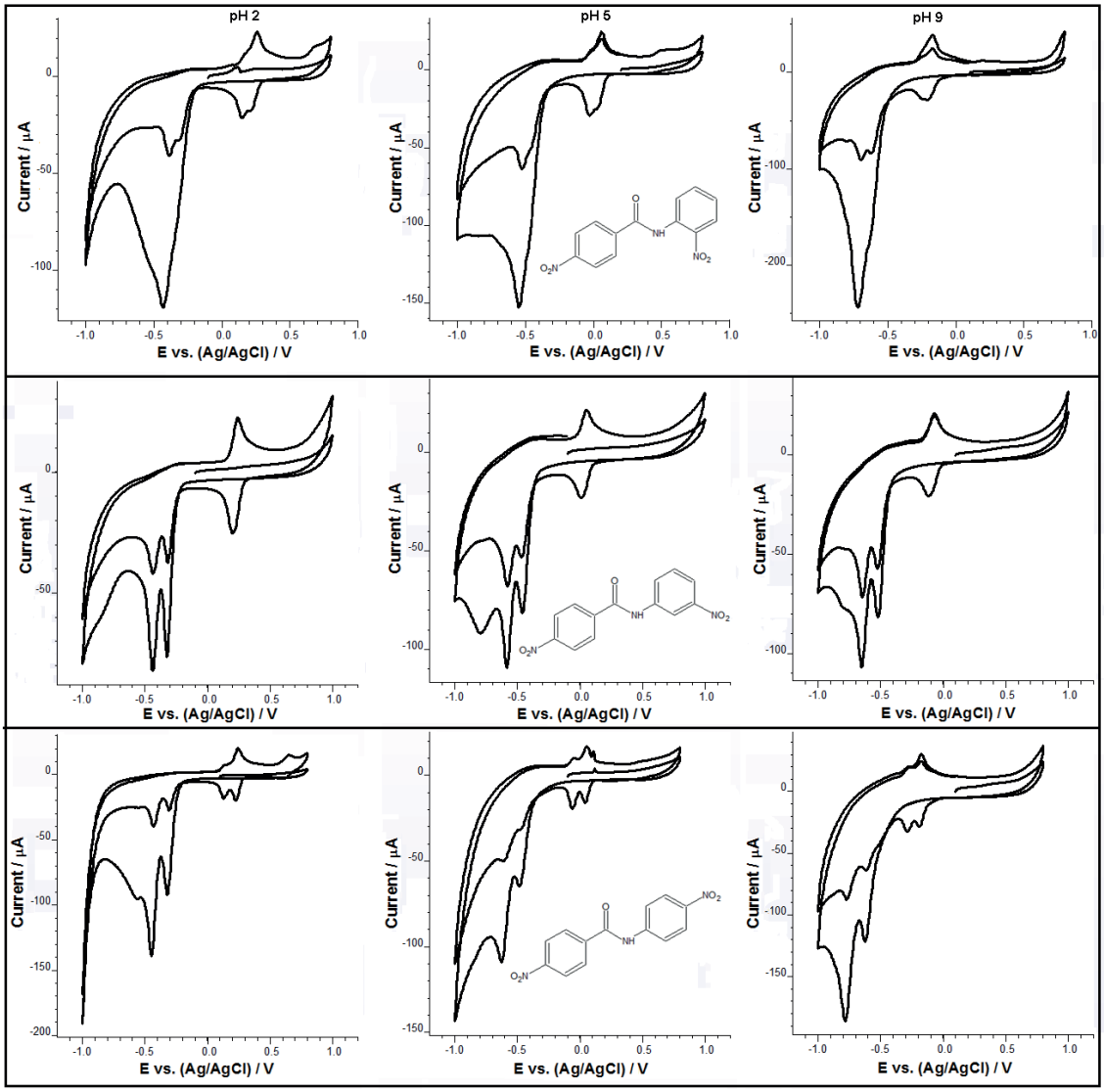

Figure S1B. Cyclic voltammograms of 0.1 mM dinitro benzamides for five successive cycles in BRBS (pH of 2, 5, and 9) containing 0.1 M KCl and 30% DMF (compounds **2**, **3**, and **4**).

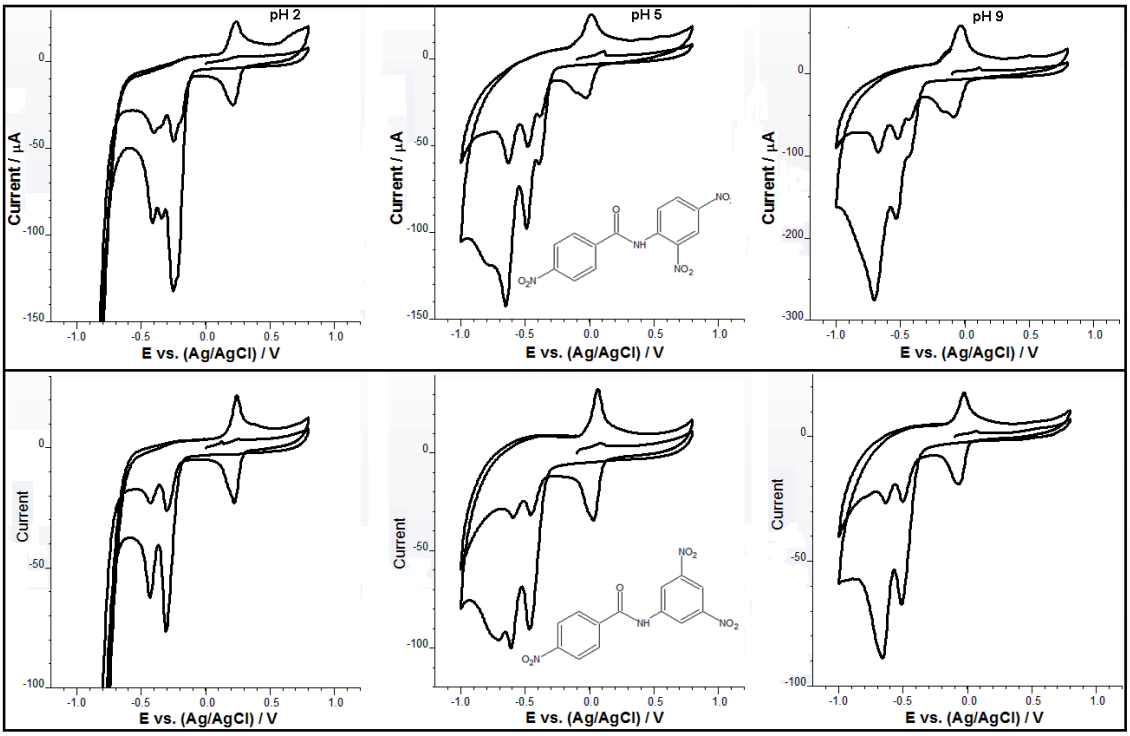

Figure S1C. Cyclic voltammograms of 0.1 mM trinitro benzamides for five successive cycles in BRBS (pH of 2, 5, and 9) containing 0.1 M KCl and 30% DMF (compounds **5** and **6**).

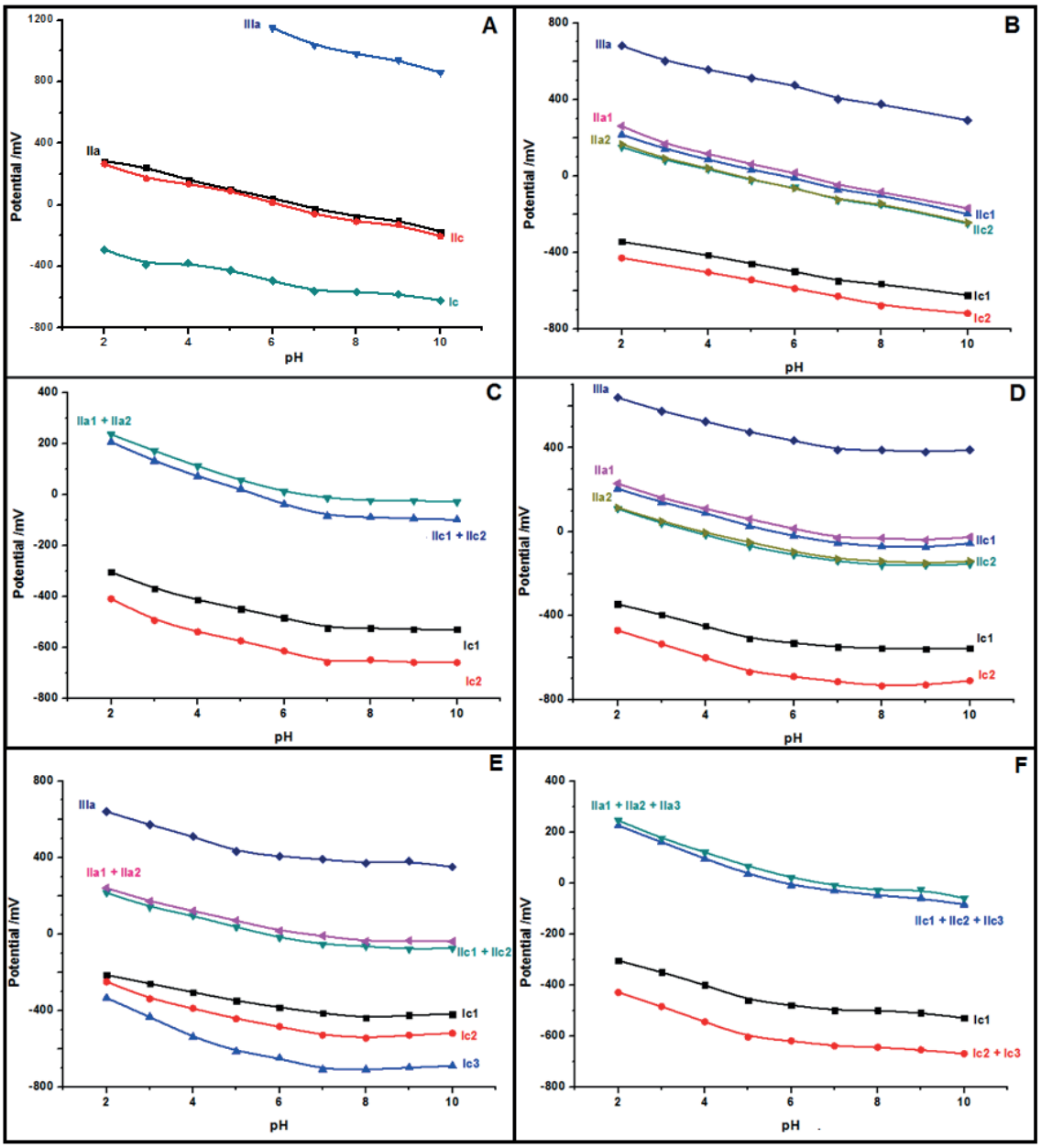

Figure S2. Plot of peak potentials of each nitro benzamide (compounds **1** (A), **2** (B), **3** (C), **4** (D), **5** (E), and **6** (F)) versus pH.

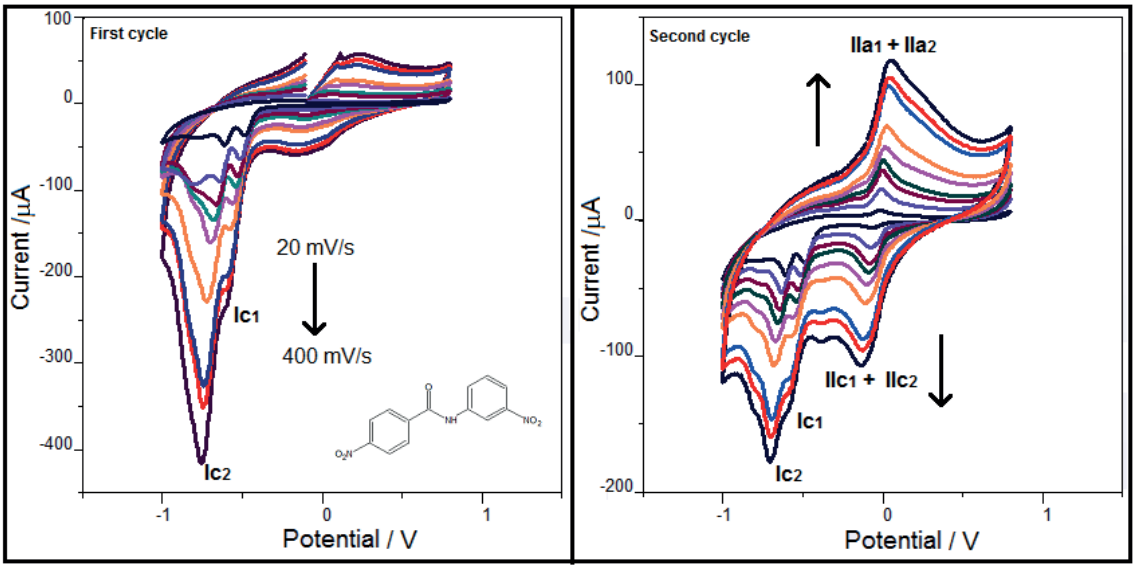

Figure S3. Cyclic voltammograms of compound **3** at different scan rates in BRBS (pH 7.0) containing 0.1 M KCl and 30% DMF on PGE.